

Spremljanje trenutne frekvenčne vsebine pri zagonu pralnega stroja

Monitoring the Instantaneous Frequency Content of a Washing Machine during Startup

Igor Simonovski - Miha Boltežar

Fourierjeva integralska transformacija je zelo uporabno orodje za analizo frekvenčnega stanja ustaljenih procesov. Pogosto pa se srečujemo tudi z neustaljenimi procesi, pri katerih običajne Fourierjeve transformacije ne moremo uporabiti. Uporabiti moramo druge metode za spremljanje frekvenčne vsebine. V tem prispevku sta predstavljeni okenska Fourierjeva transformacija in novejša zvezna valčna transformacija. Valčna transformacija je zaradi uporabe lokalno omejenih osnovnih funkcij primerna za opazovanje neustaljenih procesov. Uporabnosti omenjenih transformacij za spremljanje frekvenčne vsebine neustaljenega procesa smo ugotavljali na primeru zagona pralnega stroja. Izkazalo se je, da je zaznavnost trenutne vrtilne frekvence pri okenski Fourierjevi transformaciji slabša kakor pri zvezni valčni transformaciji. Raztros vrednosti pri okenski Fourierjevi transformaciji namreč ne omogoča zanesljive identifikacije trenutne vrtilne frekvence, ampak samo umestitev v določen frekvenčni interval. Z uporabo zvezne valčne transformacije smo bistveno zožili ta frekvenčni interval.

© 2001 Strojniški vestnik. Vse pravice pridržane.

(Ključne besede: procesi neustaljeni, transformacije Fourierjeve okenske, transformacije valčne zvezne, valčki Gaborjevi, stroji pralni)

The Fourier integral transform is a very useful tool for analyzing the frequency content of steady processes. When dealing with non-stationary processes, however, other methods for determining the frequency content must be applied. This paper deals with the windowed Fourier transform and, the more recent, wavelet transform. The windowed Fourier transform uses basic functions that have an unlimited definition range and requires multiplication of the observed process with a time-limited window function to be able to detect local non-stationarities. The wavelet transform uses basic functions that have a limited definition range for the same purpose. In this paper we compare the ability of the windowed Fourier transform and the continuous wavelet transform to monitor the frequency content of a non-stationary process—washing-machine startup. The results show that the windowed Fourier transform is inferior to the continuous wavelet transform. The wide spread of windowed Fourier transform values only makes it possible to roughly determine the instantaneous drum-spin frequency band. Using the continuous wavelet transform we were able to determine the instantaneous drum-spin frequency more accurately.

© 2001 Journal of Mechanical Engineering. All rights reserved.

(Keywords: non-stationary processes, windowed Fourier transform, continuous wavelet transform, Gabor wavelet, washing machine)

0 UVOD

Pri analizi nihanj se že vrsto let uporabljajo spektralne analize, ki temeljijo na Fourierjevi integralski transformaciji. Fourierjeva integralska transformacija je zaradi uporabe sinusnih in kosinusnih osnovnih funkcij primerna predvsem za opazovanje ustaljenih procesov. Če se v opazovanem procesu pojavijo lokalne neustaljenosti, to vpliva na Fourierjevo integralsko transformacijo pri vseh frekvencah. Ta lastnost je pri

0 INTRODUCTION

Spectral analyses, based on the Fourier integral transform, have been present in the field of vibration analysis for years. Due to the sine and cosine basic functions, the Fourier integral transform is mostly appropriate for the analysis of stationary processes. If a local non-stationary appears in the observed process its influence is spread over the Fourier integral transform values

opazovanju neustaljenih procesov nezaželena, saj nas pri teh procesih pogosto zanima trenutek pojava spremembe oziroma neustaljenosti v procesu. Prilagoditev Fourierjeve integralske transformacije za opazovanje neustaljenih procesov je okenska Fourierjeva transformacija [1]. Pri tej opazovani proces pomnožimo s časovno omejeno okensko funkcijo. Zunaj območja definirani okenske funkcije je zmnožek procesa in okenske funkcije enak nič.

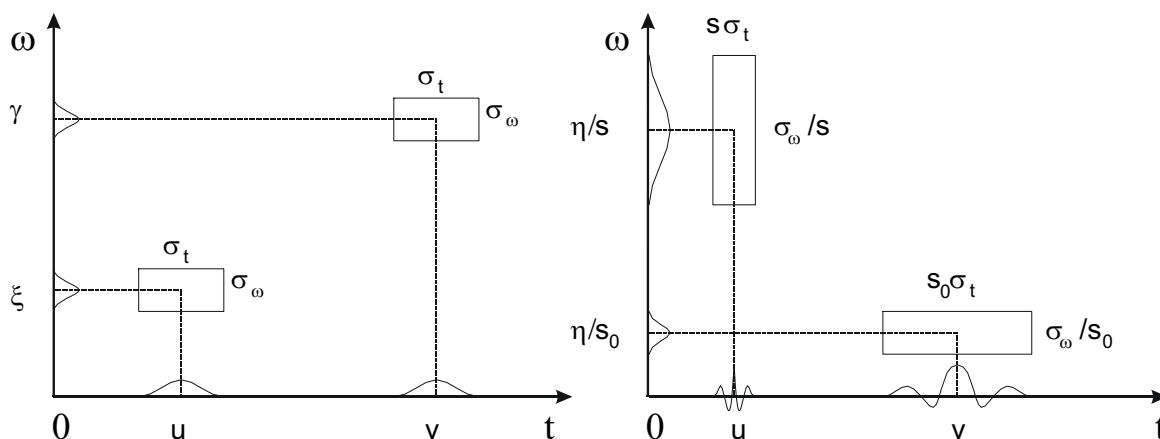
V novejšem času se je pojavila valčna transformacija, pri kateri vrednosti $f(t)$ koreliramo s skupino funkcij, katerih definicijsko območje je definirano na končnem območju $[a, b]$. Te funkcije lahko hkrati premikamo po časovni osi in skaliramo po frekvenčni osi [2]. Imenujemo jih valčki in jih označujemo s $\psi(t)$. Pomembna lastnost valčne transformacije je časovno-frekvenčno odvisen raztros valčka (sl. 1). Raztros valčka v časovnem območju je premo sorazmeren s skalo valčka, medtem ko je raztros valčka v frekvenčnem območju obratno sorazmeren s skalo valčka. Ta lastnost valčne transformacije omogoča prilagajanje frekvenčne ločljivosti. Zaradi uporabe valčnih funkcij, ki imajo lokalno omejeno definicijsko območje, je valčna transformacija občutljiva za lokalne neustaljenosti. To je zelo pomembno pri analizi neustaljenih procesov. Zato je valčna transformacija primerna za zaznavanje napak v zobniških pogonih [3], [4], strojnih napravah [5], [6] in kompozitnih ploščah [7]. Na področju dinamike se valčna transformacija uveljavlja pri identifikaciji parametrov dinamskih sistemov ([8] do [12]), izračunu časovno odvisne frekvenčne odzivne funkcije [13], linearizaciji nelinearnih sistemov [14], [15] in zaznavanju drdranja pri odrezovalnem procesu [16].

V tem prispevku primerjamo primernost okenske Fourierjeve in zvezne valčne transformacije za spremljanje frekvenčne vsebine neustaljenega procesa. Izbrani neustaljeni proces predstavlja meritev pospeškov pralne grupe pralnega stroja med zagonom. Pri dosedanjih analizah meritev pralnega stroja smo se osredotočili predvsem na spremljanje ustaljenega stanja.

at all frequencies and so the time at which the non-stationary appeared cannot be determined. To analyze a non-stationary process the windowed Fourier transform, which multiplies the observed process with a time-limited window function can be used [1]. Outside the window's definition range, the product of the process and the window function is equal to zero.

In recent years the wavelet transform has played an important role in analyzing non-stationary processes. This transform correlates the observed process, $f(t)$, with a family of functions defined on a finite interval $[a, b]$. These functions, called wavelets, $\psi(t)$, can be simultaneously translated in time and scaled in the frequency domain [2]. One important property of the wavelet transform is its varying time-frequency resolution, Figure 1. In the time domain, the wavelet spread is proportional to the wavelets' scale, while in the frequency domain the spread is inversely proportional to the wavelets' scale. This property makes it possible to vary the frequency or time resolution. Because the wavelet transform uses basic functions with a limited definition area, the wavelet transform is sensitive to the local non-stationarities. This is very important in the analysis of a non-stationary process. Thus far, the wavelet transform has been used for fault detection in gears [3], [4], machines [5], [6] and composite plates [7]. In the field of dynamics, the wavelet transform is used for parameter identification ([8] to [12]), calculating time-dependent frequency response functions [13], linearization of non-linear systems [14], [15] and chatter detection during cutting [16].

In this paper we compare the ability of the windowed Fourier transform and the continuous wavelet transform to monitor the frequency content of a non-stationary process—washing-machine startup. During startup the accelerations of the washing-machine complex have been measured. In



Sl. 1. Časovno-frekvenčna ločljivost okenske Fourierjeve (levo) in valčne transformacije (desno)
Fig. 1. The time-frequency resolution of the windowed Fourier (left) and the wavelet transform (right)

Narejene so bile spektralne analize drugega reda [18], pri katerih se je pokazalo, da je največ moči signala katerekoli merjene kinematične spremenljivke zbrane pri frekvenci ožemanja. Bispektralne analize meritev pralnega stroja so pokazale navzočnost kvadratičnih nelinearnosti [19]. Izkazalo se je, da druga, tretja in četrta harmonska niso v celoti samostojna, temveč so delno tudi posledica kvadratičnega sklapljanja faz. Narejena je bila tudi analiza odzivov modela in meritev pralnega stroja v faznem prostoru [18]. Pregled lastnega dosedanjega dela na področju analiziranja in modeliranja dinamike pralnega stroja je podan v [20] in [21].

1 TEORETIČNE OSNOVE

1.1 Okenska Fourierjeva transformacija

Fourierjeva integralska transformacija funkcije $f(t)$ je definirana kot [17]:

$$\hat{f}(\omega) = \int_{-\infty}^{+\infty} f(t) \cdot e^{-i\omega t} \cdot dt = \int_{-\infty}^{+\infty} f(t) \cdot [\cos(\omega \cdot t) - i \cdot \sin(\omega \cdot t)] \cdot dt \quad (1),$$

kjer pomeni $i = \sqrt{-1}$, ω pa krožno frekvenco v rad/s. Vrednost $\hat{f}(\omega)$ je v splošnem kompleksno število. Realni del $\hat{f}(\omega)$ opredeljuje amplitudo nihanja kosinusne funkcije pri frekvenci ω , imaginarni del $\hat{f}(\omega)$ pa amplitudo nihanja sinusne funkcije pri frekvenci ω . Kvadrat absolutne vrednosti $\hat{f}(\omega)$ poda moč funkcije $f(t)$ pri frekvenci ω . Iz izraza (1) je tudi razvidno, da lokalna neustaljenost vpliva na frekvenčno transformiranko $\hat{f}(\omega)$ pri vseh frekvencah ω . To je posledica dejstva, da je osnovna funkcija $e^{-i\omega t}$ definirana na območju $(-\infty, +\infty)$ zato h končni vrednosti integrala (1) prispevajo vsi dogodki, ne glede na čas njihovega pojava. Časovno-frekvenčna ločljivost Fourierjeve integralske transformacije je konstantna (sl. 1) [17].

Pojav okenske Fourierjeve transformacije $Sf(u, \omega)$ [1] pomeni prvi poskus omejitve vpliva oddaljenih vrednosti $f(t)$ na frekvenčno transformiranko $\hat{f}(\omega)$. Tu vrednosti $f(t)$ pomnožimo z okensko funkcijo $g_u(t) = g(t-u)$, ki je definirana na končnem območju $[a, b]$, zunaj tega območja pa je enaka nič. V skladu s tem se spremenijo integracijske meje, kar omogoči opazovanje neustaljenih pojavov.

$$Sf(u, \omega) = \int_{-\infty}^{+\infty} f(t) \cdot g_u^*(t) \cdot e^{-i\omega t} \cdot dt = \int_{meje\ g_u(t)}^b f(t) \cdot g_u^*(t) \cdot e^{-i\omega t} \cdot dt \quad (2).$$

V gornjem izrazu pomeni znak * kompleksno konjugacijo. Graf gornjega izraza pogosto imenujemo spektrogram.

V praksi običajno ne poznamo vrednosti funkcije $f(t)$ pri vseh zahtevanih časih $(-\infty, +\infty)$, temveč samo v določenem časovnem območju $[0, T]$. Funkcijo $f(t)$ lahko razširimo na celotno območje $(-\infty, +\infty)$, tako da predpostavimo, da je funkcija $f(t)$ periodična s periodo T [17]:

preliminary analyses of the washing machine dynamics we focused mainly on the stationary. Second-order spectral analyses showed that for all measured signals the drum-spin frequency has by far the highest power level [18]. Bispectra analyses revealed the presence of quadratic-order non-linearities [19]. Second, third and fourth harmonics were partially generated by quadratic phase coupling. Analyses in phase space have been applied to responses of both the model and the real system [18]. A review of our previous work relating to the analysis of washing-machine non-linear dynamics can be found in [20] and [21].

1 THEORETICAL FOUNDATIONS

1.1 The windowed Fourier transform

The Fourier integral transform of the function is defined as [17]:

where $i = \sqrt{-1}$ and ω is the circular frequency in rad/s. The value of $\hat{f}(\omega)$ at a certain frequency ω is, in general, a complex number. The real and imaginary parts of $\hat{f}(\omega)$ represent the amplitude of the sine and cosine functions, oscillating at frequency ω . The absolute value of $\hat{f}(\omega)$ squared is the power at the frequency ω . It is evident from (1) that the local non-stationary affects the frequency transform of $\hat{f}(\omega)$ at all frequencies ω , a consequence of the basic function $e^{-i\omega t}$. Since its definition interval is $(-\infty, +\infty)$, the integration is carried out over this whole interval. The time-frequency resolution of the Fourier integral transform is constant and is presented in Figure 1, [17].

The windowed Fourier transform reduces the influence of time-distant events on the frequency transform, $\hat{f}(\omega)$, by multiplying the $f(t)$ with the time-limited window function $g_u(t) = g(t-u)$. The window function, $g_u(t)$, is defined on a finite interval $[a, b]$ and is equal to zero outside this interval. As a consequence, the integral limits change, which makes the windowed Fourier transform useful for observing non-stationary processes.

The symbol * in expression (2) denotes a complex conjugation. The graph of $Sf(u, \omega)$ is often referred to as a spectrogram.

In practice, the function $f(t)$ is usually only known in the time interval $[0, T]$. In this case $f(t)$ can be extended to the interval $(-\infty, +\infty)$ with periodization by T [17]:

$$f(t) = f(t \pm k \cdot T), \quad 0 \leq t \leq T, \quad k = 0, 1, 2, \dots \quad (3)$$

Vsako periodično funkcijo $f(t)$ s periodo T in definirano na območju $[0, T]$ pa lahko izrazimo z naslednjo vrsto:

Any periodical function $f(t)$ with period T and defined in the interval $[0, T]$ can be expressed with the following series:

$$f(t) = a_0 + 2 \cdot \sum_{k=1}^{k=\infty} a_k \cdot \cos\left(\frac{2 \cdot \pi \cdot k \cdot t}{T}\right) + b_k \cdot \sin\left(\frac{2 \cdot \pi \cdot k \cdot t}{T}\right), \quad 2 \cdot \pi \cdot k \cdot t = \omega \quad (4)$$

pri čemer so koeficienti a_k in b_k :

where coefficients a_k and b_k are:

$$a_k = \frac{1}{T} \cdot \int_0^T f(t) \cdot \cos\left(\frac{2 \cdot \pi \cdot k \cdot t}{T}\right) \cdot dt, \quad k \geq 0 \quad (5)$$

$$b_k = \frac{1}{T} \cdot \int_0^T f(t) \cdot \sin\left(\frac{2 \cdot \pi \cdot k \cdot t}{T}\right) \cdot dt, \quad k \geq 0 \quad (6)$$

Izraza (5) in (6) lahko združimo, če uporabimo kompleksni zapis:

Expressions (5) and (6) can be combined by complex notation:

$$X_k = a_k - i \cdot b_k \quad (7)$$

Ker velja:

Since:

$$e^{-i \cdot \left(\frac{2 \cdot \pi \cdot k \cdot t}{T}\right)} = \cos\left(\frac{2 \cdot \pi \cdot k \cdot t}{T}\right) - i \cdot \sin\left(\frac{2 \cdot \pi \cdot k \cdot t}{T}\right) \quad (8)$$

lahko zapišemo naslednji izraz za X_k :

the following expression can be written:

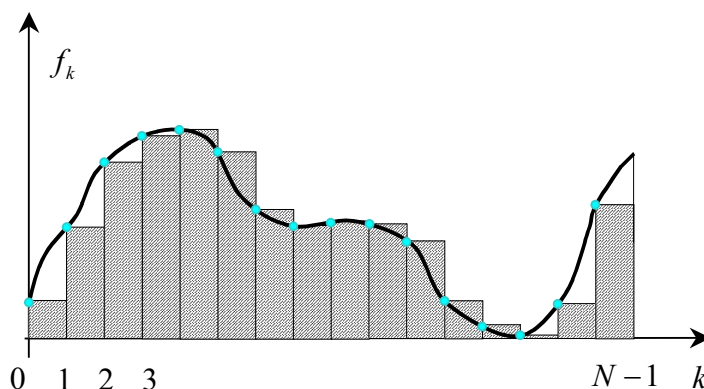
$$X_k = \frac{1}{T} \int_0^T x(t) \cdot e^{-i \cdot \left(\frac{2 \cdot \pi \cdot k \cdot t}{T}\right)} \cdot dt, \quad k \geq 0 \quad (9)$$

V praksi običajno ne poznamo vseh vrednosti $f(t)$. Opazovani proces vzorčimo s frekvenco vzorčenja $f_s = 1/\Delta t$, tako da poznamo samo vrednosti pri diskretnih časih $f_k = f(k \cdot \Delta t)$, $k=0, 1, 2, \dots, N-1$. Oznaka Δt pomeni časovni razmik med dvema sosednjima diskretnima točkama, N pa število točk diskretizacije, sl 2. Integral (9) izračunamo z numerično integracijo, kjer periodo T zapišemo kot $T=N \cdot \Delta t$:

In practice $f(t)$ is usually known only for discrete time indexes. The observed process $f(t)$ is sampled with the sampling frequency $f_s = 1/\Delta t$, therefore only the values $f_k = f(k \cdot \Delta t)$, $k=0, 1, 2, \dots, N-1$ are known. The symbol N denotes the number of sampled points while Δt stands for the time delay between sampled points, Figure 2. The integral (9) is calculated using numerical integration, where period T is written as $T=N \cdot \Delta t$:

$$X_k = \frac{1}{T} \cdot \sum_{j=0}^{j=N-1} x_j \cdot e^{-i \cdot \left(\frac{2 \cdot \pi \cdot k \cdot (j \cdot \Delta t)}{T}\right)} \cdot \Delta t \quad (10)$$

$$X_k = \frac{1}{N} \cdot \sum_{j=0}^{j=N-1} x_j \cdot e^{-i \cdot \left(\frac{2 \cdot \pi \cdot k \cdot j}{N}\right)} \quad (11)$$



Sl. 2. Diskretizacija zvezne funkcije
Fig. 2. Discretized continuous function

Izraz (11) poznamo pod imenom “diskretna Fourierjeva transformacija”. Če se na začetku signala $f(t)$ pojavi neustaljenost, ki kasneje izgine, ta neustaljenost vpliva na vse člene a_k, b_k . Ta zakonitost izhaja iz izrazov (5) in (6). Členi a_k in b_k pomenijo diskretno Fourierjevo transformirano diskretiziranega signala f_k . Začasna neustaljenost v signalu torej vpliva na koeficiente celotne diskretne Fourierjeve transformacije. Ta lastnost otežuje analizo lokalnih lastnosti pojava, zaradi česar je Fourierjeva transformacija primerna predvsem za analizo ustaljenih pojavov.

1.2 Zvezna valčna transformacija

Valček $\psi(t)$ je normirana funkcija z nično povprečno vrednostjo:

$$\int_{-\infty}^{+\infty} |\psi(t)|^2 \cdot dt = 1 \quad (12),$$

$$\int_{-\infty}^{+\infty} \psi(t) \cdot dt = 0 \quad (13).$$

Skupino valčnih funkcij, ki jih uporabimo pri zvezni valčni transformaciji, dobimo s skaliranjem valčka $\psi(t)$ po frekvenčni osi s koeficientom “s” (skalirni koeficient) in s premikanjem valčka po časovni osi s parametrom premika “u”. Skaliran in premaknjen valček označimo s $\psi_{u,s}(t)$:

$$\psi_{u,s}(t) = \frac{1}{\sqrt{s}} \cdot \psi\left(\frac{t-u}{s}\right) \quad (14).$$

Tako skaliran valček ohrani lastnost normiranosti. Na časovni osi je središče $\psi_{u,s}(t)$ pri “u”, frekvenčna razsežnost pa je sorazmerna s skalo “s”. Frekvenčno transformacijo valčka $\psi_{u,s}(t)$ dobimo z uporabo pravil o translaciji in skaliranju Fourierjevih transformirank:

$$\hat{\psi}_{u,s}(\omega) = e^{-i \cdot u \cdot \omega} \cdot \sqrt{s} \cdot \hat{\psi}(s \cdot \omega) \quad (15),$$

kjer $\hat{\psi}(\omega)$ pomeni Fourierjevo transformacijo nepremaknjene in neskaliranega valčka $\psi(t)$. Zvezna valčna transformacija $Wf(u,s)$ je definirana kot:

$$Wf(u,s) = \int_{-\infty}^{+\infty} f(t) \cdot \psi_{u,s}^*(t) \cdot dt = \int_{-\infty}^{+\infty} f(t) \cdot \frac{1}{\sqrt{s}} \cdot \psi^*\left(\frac{t-u}{s}\right) \cdot dt \quad (16).$$

Graf gornjega izraza pogosto imenujemo skalogram. Valček $\psi_{u,s}(t)$ je funkcija, ki je definirana na končnem območju [a, b], zato je valčna transformacija občutljiva na lokalne neustaljenosti. Če se v funkciji $f(t)$ v določenem trenutku pojavi prehodni pojav, se bo pokazal le na valčni transformiranki v okolici tega pojava. Prehodni pojav ne bo vplival na valčno transformiranko pri časovnih vrednostih “u”, ki so oddaljene od trenutka njegovega pojava in trajanja. Valčne funkcije so lahko realne ali kompleksne. Realne valčne funkcije uporabljamo, če želimo zaznati močne prehodne pojave. Kompleksni valčki so primerni za časovno opazovanje frekvenčnih sprememb v prehodnih pojavih.

Expression (11) is known as the “discrete Fourier transform” (DFT). Coefficients a_k and b_k can therefore be obtained from classical DFT routines. If non-stationary appears at the beginning of the signal and later vanishes, it influences all coefficients a_k and b_k . This property is the result of integrating over the whole period T ((5) and (6)) and makes it difficult to analyze local events in the signal. Consequently, the Fourier transform is used primarily for analyzing stationary processes.

1.2 The continuous wavelet transform

The wavelet $\psi(t)$ is a normalized function with an average value of zero:

The continuous wavelet transform uses a family of wavelet functions. Scaling a wavelet function $\psi(t)$ by “s” and translating it by “u” creates this family of wavelet functions. These two coefficients are called the scaling factor and the translation parameter, respectively. The scaled and translated wavelet is denoted as $\psi_{u,s}(t)$:

and remains normalized. On the time scale $\psi_{u,s}(t)$ is centered at “u”. The frequency resolution is proportional to scale “s”. The frequency transform of the wavelet $\psi_{u,s}(t)$ is obtained from Fourier transform rules for translation and scaling:

where $\hat{\psi}(\omega)$ represents the Fourier transform of untranslated and unscaled $\psi(t)$. The continuous wavelet transform $Wf(u,s)$ is defined as:

The graph of $Wf(u,s)$ is often referred to as a scalogram. Because the wavelet $\psi_{u,s}(t)$ is defined on a finite interval [a, b], the continuous wavelet transform is sensitive to local events (non-stationarities). The local transient reflects on the continuous wavelet transform only when the transient appears and only for the duration of the transient. The continuous wavelet transform that is distanced in time from a local transient is unaffected by it. Wavelet functions can be real or complex, real wavelets are often used to detect sharp signal transitions. Measuring the time evolution of frequency transients requires the use of a complex wavelet which can separate amplitude and phase components.

Inverzna zvezna valčna transformacija je definirana kot:

$$f(t) = \frac{1}{C_\psi} \int_0^{+\infty} \int_{-\infty}^{+\infty} Wf(u, s) \cdot \frac{1}{\sqrt{s}} \cdot \psi\left(\frac{t-u}{s}\right) \cdot du \cdot \frac{ds}{s^2} \quad (17),$$

pri čemer je:

$$C_\psi = \int_0^{+\infty} \frac{|\hat{\psi}(\omega)|}{\omega} \cdot d\omega < +\infty \quad (18).$$

Dodatno se zahteva, da je valček $\psi_{u,s}(t)$ realna funkcija [17].

The inverse continuous wavelet transform can be defined as:

Expression (17) requires the wavelet $\psi_{u,s}(t)$ to be a real function [17].

1.3 Izračun zvezne valčne transformacije

Obravnavajmo diskreten signal z N točkami:

$$f_k = f(k \cdot \Delta t), \quad k = 0, 1, 2, \dots, N-1 \quad (19).$$

Signal f_k je poznan samo v časovnem območju:

$$t_0 = 0 \leq t \leq (N-1) \cdot \Delta t = t_1 \quad (20),$$

zato se meje integracije v izrazu za zvezno valčno transformacijo spremenijo v:

$$Wf(u, s) = \int_{t_0}^{t_1} f(t) \cdot \psi_{u,s}^*(t) \cdot dt = \int_0^{(N-1)\Delta t} f(t) \cdot \frac{1}{\sqrt{s}} \cdot \psi\left(\frac{t-u}{s}\right) \cdot dt \quad (21).$$

Za določen vnaprej izbran časovi razmik "u=n·Δt" in skalo "s" izračunamo gornji izraz z numerično integracijo:

$$Wf(n \cdot \Delta t, s) = \sum_{m=0}^{m=N-1} f(m \cdot \Delta t) \cdot \frac{1}{\sqrt{s}} \cdot \psi^*\left(\frac{m \cdot \Delta t - n \cdot \Delta t}{s}\right) \cdot \Delta t \quad (22),$$

pri čemer smo predpostavili, da imata diskretni signal f_k in valčna funkcija $\psi_{u,s}(t)$ enako dolžino na časovni osi. Če označimo:

$$\psi_{k,s}^* = \frac{1}{\sqrt{s}} \cdot \psi^*\left(\frac{k \cdot \Delta t}{s}\right) \quad (23),$$

lahko zapišemo numerično integracijo kot:

$$Wf(n \cdot \Delta t, s) = \Delta t \cdot \sum_{m=0}^{m=N-1} f_m \cdot \psi_{m-n,s}^* \quad (24).$$

Izraz (24) zelo spominja na diskretno konvolucijo. S spremembo indeksov vektorja $\psi_{m-n,s}^*$ lahko gornji izraz spremenimo tako, da ga izračunamo z diskretno konvolucijo. V vektorju $\psi_{m-n,s}^*$ obrnemo vrstni red indeksov. Naredimo nov vektor $\bar{\psi}_{k,s}$, katerega prvi element je zadnji element vektorja $\psi_{m-n,s}^*$. Drugi element vektorja $\psi_{m-n,s}^*$ je predzadnji element vektorja $\psi_{m-n,s}^*$ in tako naprej.

$$\bar{\psi}_{k,s} = \psi_{N-1-k,s}^*, \quad k = 0, 1, 2, \dots, N-1 \quad (25).$$

Končni izraz za izračun zvezne valčne transformacije se torej glasi:

1.3 Calculation of the continuous wavelet transform

Suppose we have a discrete signal with N points:

Consequently, integration limits in the expression for the continuous wavelet transform change to:

For the given translation "u=n·Δt" and scale "s", expression (21) is calculated using numerical integration:

where the assumption has been made that the discrete signal f_k and the wavelet function $\psi_{u,s}(t)$ both have the same length on the time scale. We denote:

and the numerical integration can be written as:

Expression (24) is similar to the expression for discrete convolution. If we change the indexes of vector $\psi_{m-n,s}^*$, expression (24) can be adapted in such a way that we can calculate it using discrete convolution. We take vector $\psi_{m-n,s}^*$ and reverse its indexes. We denote the newly obtained vector as $\bar{\psi}_{k,s}$.

Finally, the expression for calculating the continuous wavelet transform using discrete convolution is:

$$Wf(n \cdot \Delta t, s) = \Delta t \cdot \sum_{m=0}^{m=N-1} f_m \cdot \bar{\psi}_{n-m, s} = \Delta t \cdot f \otimes \bar{\psi}_{n, s} \quad (26).$$

Konvolucija v časovnem območju postane množenje v frekvenčnem območju. Za prehod v frekvenčno območje lahko uporabimo algoritem hitre Fourierjeve transformacije. Pri izbranem časovnem razmiku "u" in skali "s" obrnemo vrstni red indeksov vektorja $\hat{\psi}_{m-n, s}^*$, da dobimo vektor $\bar{\psi}_{n-m, s}$. Če je valčna funkcija pri "u=0" simetrična, zamenjava indeksov ne spremeni ničesar. V tem primeru lahko to zamenjavo preskočimo. Nato izračunamo hitro Fourierjevo transformacijo vektorjev f_m in $\bar{\psi}_{n-m, s}$ ter jih medsebojno pomnožimo. Na koncu dobimo zvezno valčno transformacijo pri določenem časovnem razmiku "u" in skali "s" z obratno Fourierjevo transformacijo pomnoženih vektorjev. Zadnji korak je še množenje s Δt , ki pa ga večina avtorjev ne izvede. Postopek ponovimo pri preostalih skalah "s".

Because convolution in the time domain is multiplication in the frequency domain, convolution is carried out in the frequency domain. We can recapitulate the procedure for calculating the continuous wavelet transform. First we select the translation "u" and "s". Next the indexes of vector $\hat{\psi}_{m-n, s}^*$ are changed according to (25) to obtain vector $\bar{\psi}_{n-m, s}$. If the wavelet function is symmetrical at "u=0" the reversal of indexes is not necessary. The Fourier discrete transform of vectors f_m and $\bar{\psi}_{n-m, s}$ is calculated. Fourier transforms of these two vectors are then multiplied index by index to calculate the convolution in the frequency domain. An inverse Fourier transform is performed to obtain the convolution in the time domain. Lastly, we must multiply the resulting vector by Δt , although many authors omit this step. The procedure is repeated for other scales "s".

1.4 Gaborjev valček

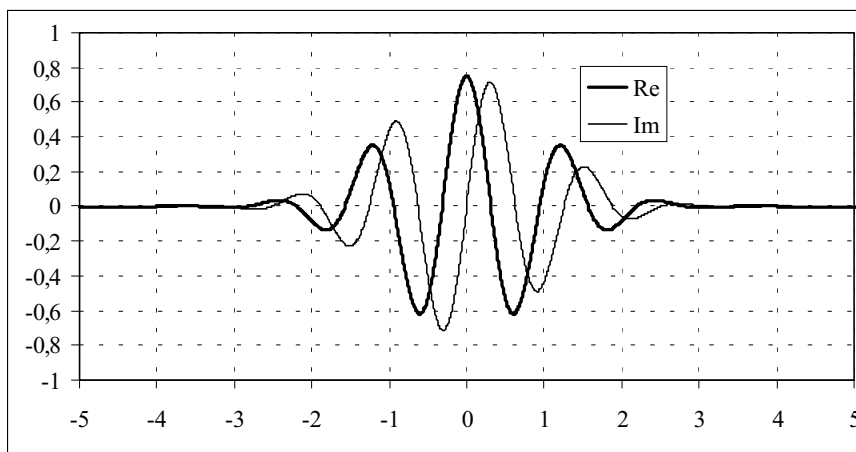
Gaborjev valček (sl. 3) dobimo z množenjem Gaussove okenske funkcije in $e^{i \cdot \eta \cdot t}$:

$$w_{Gauss}(t, \sigma) = \frac{1}{(\sigma^2 \cdot \pi)^{\frac{1}{4}}} \cdot e^{-\frac{t^2}{2 \cdot \sigma^2}} \quad (27),$$

$$\psi_{Gabor}(t, \sigma, \eta) = \frac{1}{(\sigma^2 \cdot \pi)^{\frac{1}{4}}} \cdot e^{-\frac{t^2}{2 \cdot \sigma^2}} \cdot e^{i \cdot \eta \cdot t} \quad (28).$$

1.4 The Gabor wavelet

The Gabor wavelet, Figure 3, is obtained by multiplying the Gaussian windows by $e^{i \cdot \eta \cdot t}$:



Sl. 3. Gaborjev valček
Fig. 3. The Gabor wavelet

Koeficient η je odvisen od frekvence vzorčenja in izbrane začetne skale. Skaliran in premaknjen Gaborjev valček dobimo iz izraza (14):

Coefficient η depends on the sampling frequency and the selected initial scale. The scaled and translated Gabor wavelet is obtained from (14):

$$\psi_{Gabor_{u, s}}(t, \sigma, \eta) = \frac{1}{\sqrt{s}} \cdot \frac{1}{(\sigma^2 \cdot \pi)^{\frac{1}{4}}} \cdot e^{-\left(\frac{t-u}{s}\right)^2} \cdot \frac{1}{2 \cdot \sigma^2} \cdot e^{i \cdot \eta \cdot \frac{t-u}{s}} \quad (29).$$

Gaborjev valček spada med analitične valčke. Za Gaborjev valček lahko dobimo povezavo

The Gabor wavelet belongs to the family of analytical wavelets. The relationship between the

med skalo in frekvenco iz Fourierjeve integralske transformacije skaliranega in premaknjene Gaborjevega valčka (22):

$$\hat{\psi}_{Gabor_{u,s}}(\omega, \sigma, \eta) = (4 \cdot \pi \cdot \sigma^2 \cdot s^2)^{\frac{1}{4}} \cdot e^{-i \cdot \omega \cdot u} \cdot e^{-\left(\omega - \frac{\eta}{s}\right)^2 \cdot \frac{\sigma^2 \cdot s^2}{2}} \quad (30).$$

Velja torej naslednja povezava med skalo in frekvenco:

$$\omega = \frac{\eta}{s}, f = \frac{\eta}{2 \cdot \pi \cdot s} \quad (31).$$

Pri diskretnih signalih mora biti izpolnjen Nyquistov kriterij:

$$f_{\max} \leq \frac{1}{2 \cdot \Delta t} = \frac{f_s}{2} \quad (32),$$

iz česar lahko izračunamo vrednost koeficienta η :

$$\eta = \frac{s_{\min} \cdot \pi}{\Delta t} \quad (33),$$

pri čemer s_{\min} izberemo glede na potrebno časovno oziroma frekvenčno ločljivost (sl. 1).

scale and the frequency can be obtained from the Fourier integral transform of the scaled and translated Gabor wavelet (22):

The relationship between the scale and frequency is:

When using discretized signals, the Nyquist criterion must be satisfied:

and the value of the η coefficient can be calculated:

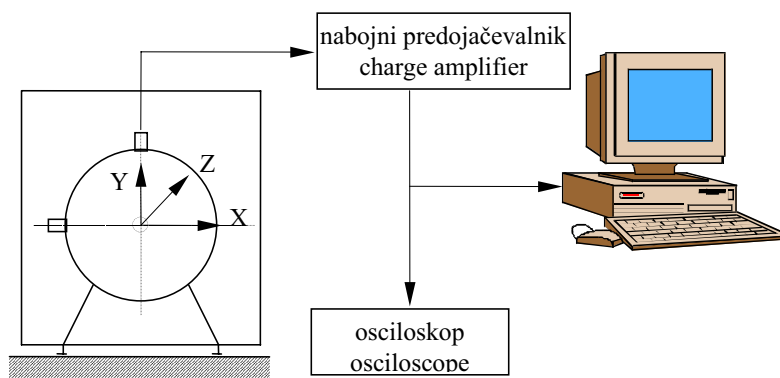
Parameter s_{\min} is selected in accordance with the desired time or frequency resolution, see Figure 1.

2 ANALIZA ZAGONA PRALNEGA STROJA

Pri zagonu pralnega stroja smo merili pospeške pralne grupe v vertikalni in horizontalni smeri (sl. 4). Pralna grupa je del pralnega stroja ter jo sestavljajo kad z rotirajočim bobnom, dodana utež, elektromotor in vibroizolacija. V bobnu je na največjem polmeru pritrjena ekscentrična masa. Pri vrtenju bobna povzroči ekscentrična masa neuravnoteženost, s katero lahko simuliramo najslabšo mogočo porazdelitev perila pri pranju. Podrobnosti o meritvah so podane v [18] in [19]. Uporabljena je bila frekvenca vzorčenja $f_s=1000$ Hz. Število diskretnih točk je bilo 30000, kar pomeni časovno 30 s. Izmerjenim 30000 točkam smo na koncu dodali še 2768 diskretnih ničel, tako da smo dobili celotno dolžino $32768=2^{15}$ diskretnih točk. Pri zagonu smo spremljali časovno spreminjanje frekvenčne slike pospeškov pralne grupe pralnega stroja. Časovno spreminjajočo se frekvenčno sliko smo dobili iz pospeškov z izračunom okenske Fourierjeve (spektrogram) in zvezne valčne

2 WASHING-MACHINE STARTUP ANALYSIS

Horizontal and vertical accelerations of a washing-machine complex were measured, Figure 4. The washing-machine complex is made up of: the tub in which the drum is rotating; additional weights; the electromotor attached to the tub and the suspension arms holding the tub as vibroisolation. In the drum of the washing-machine complex an excentric mass was fixed at the maximum radius, to unbalance the rotating parts and simulate the worst possible laundry distribution. Details of the measurements are given in [18] and [19]. A sampling frequency of $f_s=1000$ Hz was used and the length of all measurements was 30000 discrete points, which is equivalent to 30 s. 2768 discrete zeroes were appended to the 30000 measured points, giving a final length of $32768=2^{15}$ discrete points. During startup, the spectral content of the washing-machine accel-



Sl. 4. Shema merilne verige pralnega stroja
Fig. 4. The experimental set-up

transformacije (skalogram). Spremljanje frekvenčne slike z dvema različnima integralnima transformacijama je omogočilo vpogled v razlike med obema izračunoma. Ker je okenska Fourierjeva transformacija v primerjavi z valčno transformacijo že po svoji naravi manj primerna za opazovanje neustaljenih pojavov, smo okensko Fourierjevo transformacijo izračunali na dva načina:

- Z uporabo 512 vhodnih točk v rutini FFT, brez dodajanja ničel. Frekvenčna ločljivost pri teh izračunih je $\Delta f = 1,953$ Hz.
- Z uporabo $512 + 1536 = 2048 = 2^{11}$ vhodnih točk v rutini FFT. 512 točk je predstavljalo točke meritve, preostalih 1536 točk pa je bilo ničel. Ničle smo dodali z namenom izboljšanja frekvenčne ločljivosti. Frekvenčna ločljivost pri teh izračunih je $\Delta f = 0,488$ Hz.

Uporabili smo Gaussovo okensko funkcijo, ki smo jo premikali po signalu meritve za 10 diskretnih točk v smeri naraščanja časovnih indeksov. Zvezno valčno transformacijo smo izračunali z uporabo Gaborjevega valčka, ki nastane iz Gaussove okenske funkcije. Zaradi primerljivosti so spektrogrami in skalogrami izračunani z istima frekvenčnima ločljivostima (1,953 in 0,488 Hz). Podatki o izračunu spektrogramov so podani v preglednici 1, podatki o izračunu skalogramov pa v preglednici 2.

erations was monitored by calculating the windowed Fourier transform (spectrograms) and the continuous wavelet transform (scalograms). By using two different approaches we were able to compare both methods. The windowed Fourier transforms were calculated with two frequency resolutions:

- Number of points in the FFT procedure 512, no zero padding. Frequency resolution $\Delta f = 1.953$ Hz;
- Number of points in the FFT procedure $512 + 1536 = 2048 = 2^{11}$, 512 measured points and 1536 zero padded points. Frequency resolution $\Delta f = 0.488$ Hz.

The Gaussian window function was used. Window functions were time-shifted by 10 discrete points in the direction of increasing time indexes. Continuous wavelet transforms were calculated using the Gabor wavelet, which comes from the Gaussian window function. Spectrograms and scalograms were calculated with two frequency resolutions (1.953 and 0.488 Hz). Details of the spectrogram and scalogram calculations are given in Tables 1 and 2.

Preglednica 1. Podatki o parametrih izračuna spektrogramov

Tabel 1. Spectrogram calculation data

	Spektrogram $\Delta f = 1,953$ Hz Spectrogram	Spektrogram $\Delta f = 0,488$ Hz Spectrogram
okenska funkcija window function	Gaussova Gaussian	Gaussova Gaussian
zamik okenske funkcije window function shift	10 [diskretne točke] 10 [discrete points]	10 [diskretne točke] 10 [discrete points]
širina okenske funkcije brez ničel window function width without zeroes	512	512
število dodanih ničel added zeroes	0	1536
skupno število točk overall number of points	512	2048
frekvenčna ločljivost frequency resolution	1,953 Hz	0,488 Hz

Preglednica 2. Podatki o parametrih izračuna skalogramov

Tabel 2. Scalogram calculation data

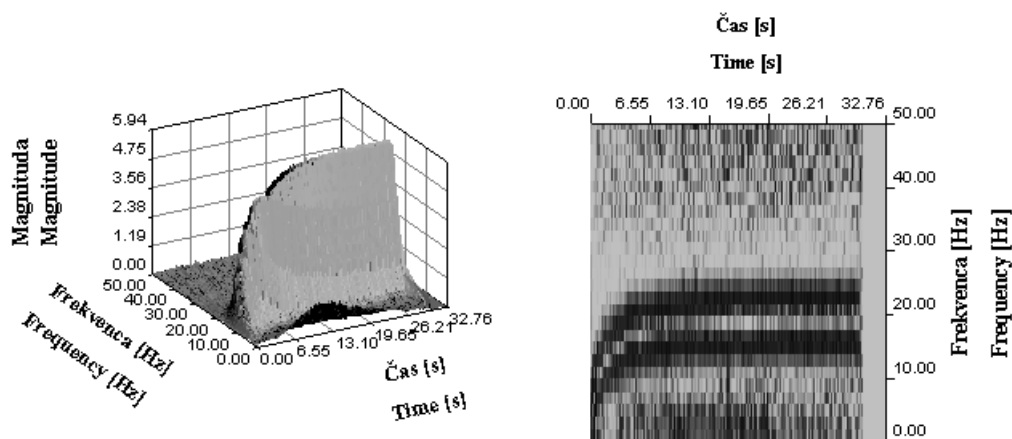
	Skalogram $\Delta f = 1,953$ Hz Scalogram	Skalogram $\Delta f = 0,488$ Hz Scalogram
valček wavelet	gabor	gabor
s_{\min}	2	2
σ	1,5	1,5
spodnja meja računanege frekvenčnega območja lower frequency bound	2 Hz	2 Hz
zgornja meja računanege frekvenčnega območja higher frequency bound	50 Hz	50 Hz
frekvenčna ločljivost frequency resolution	1,953 Hz	0,488 Hz

2.1 Primerjava spektrogramov in skalogramov

Na slikah 5 do 8 so prikazani spektrogrami in skalogrami horizontalnih pospeškov pralne grupe pralnega stroja pri zagonu. Slika 5 prikazuje magnitudo spektrograma. Zaradi preglednosti je prikazano le frekvenčno območje od 0 do 50 Hz. Levi del slike prikazuje skalogram v prostoru, desni del pa tlorisno projekcijo. Frekvenčna ločljivost je 1,953 Hz. Na sliki lahko vidimo greben, katerega magnituda in frekvenca s časom naraščata. Greben je dejansko magnituda koeficientov Fourierjeve transformacije, sestavljajo ga močnostni spektri izračunani pri določenih časovnih indeksih. Zaradi zagona frekvenca s časom narašča. Amplituda nihanja se povečuje, posledično pa se večajo tudi koeficienti izračunane okenske Fourierjeve transformacije. Poleg povečevanja frekvence zaganjanja drugih zaznavnih frekvenčnih komponent ni opaziti. Tu je treba poudariti, da je magnitudna os prikazana na linearni in ne na logaritemski skali. Po 30 s lahko opazimo, da je magnituda spektrograma enaka nič. To je posledica dejstva, da je imela uporabljena meritev le 30000 točk, kar časovno ustreza 30 s. Za 30000 diskretnimi točkami pa smo v signal dodali dodatne ničle, tako da smo dobili skupno dolžino signala 32768 točk. Po 30 s torej ni več amplitude nihanj, magnitudni spektri morajo biti enaki nič pri vseh frekvencah, to pa lahko tudi vidimo na izračunanih spektrogramih. Zaradi uporabe $2^{15}=32768$ točk smo lahko za izračun skalogramov uporabili postopek hitre Fourierjeve transformacije, kar je pospešilo numerični izračun. Opazimo lahko, da je slika tlorisne projekcije spektrogramov zelo nejasna. Ta nejasnost je posledica slabe frekvenčne ločljivosti in uporabe sinusnih (kosinusnih) funkcij, ki jih uporablja Fourierjeva transformacija za dekompozicijo signala. Raztros moči na sosednje frekvence bi lahko zmanjšali z boljšo izbiro okenske funkcije, vendar bi s tem zmanjšali primerljivost spektrograma in skalograma. Tako pa smo pri okenski Fourierjevi in zvezni valčni

2.1 Comparison of spectrograms and scalograms

Figures 5 through 8 show the spectrograms and scalograms of the washing-machine complex's horizontal accelerations during startup. Figure 5 depicts the spectrogram magnitude. For clarity reasons only the frequency range 0 to 50 Hz is presented. The left part of the picture shows a surface plot presentation while the right part shows a 2D plot of the spectrogram. The frequency resolution is 1.953 Hz. A ridge representing the maximum value of the magnitude of the wavelet function at an appropriate scale (frequency) and translation (time index) can be clearly seen. Due to the startup, the amplitude of vibrations and the revolutions of the drum are increasing. The spectrogram and the ridge represent the magnitude of the coefficients of the Fourier transform at a given time index. The spectrogram magnitude is therefore directly dependent upon the amplitude of the vibrations. The increase in the amplitudes of vibrations manifests itself as the increasing magnitude of the ridge. The frequency of the ridge represents the instantaneous frequency with the highest power. Since this equals the rotating frequency of the drum, the ridge frequency represents the instantaneous rotation frequency of the drum. With the exception of the drum frequency, other frequencies do not have significant power. We must point out, however, that the magnitude is shown on a linear and not on a logarithmic scale. After 30 s the magnitude of the spectrogram vanishes. This is because after 30 s vibrations were no longer recorded and zeros were added into the signal. These zeros state that in the time period after 30 s, the amplitude of the vibrations is zero. The spectrogram therefore must be zero and this can be seen in the figures. Because $2^{15}=32768$ discrete points were used for calculating the spectrogram we were able to use the fast Fourier transform procedure which significantly reduced the calculation time. The 2D plot of the spectrogram is



Sl. 5. Spektrogram, frekvenčna ločljivost 1,953 Hz
Fig. 5. The spectrogram, frequency resolution 1.953 Hz

transformaciji uporabili zelo sorodno Gaussovo okensko funkcijo in Gaborjevo valčno funkcijo.

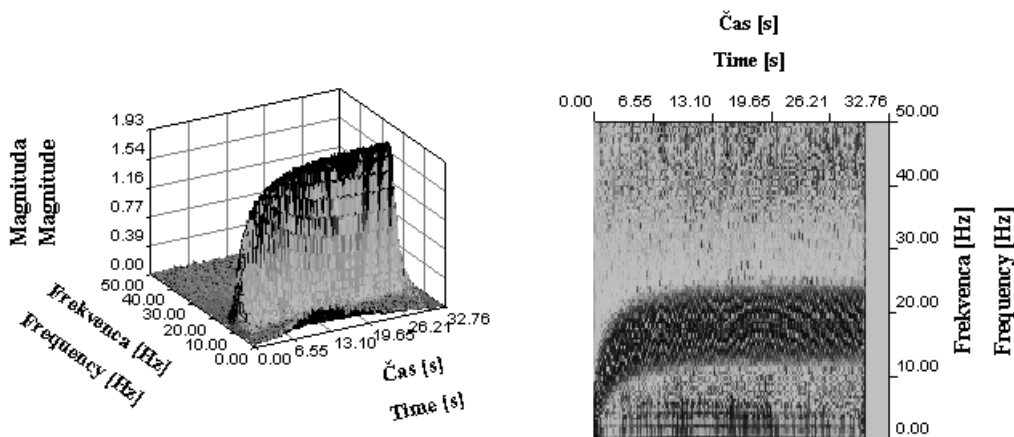
Frekvenčno ločljivost smo skušali izboljšati tako, da smo širino vsake okenske funkcije povečali na 2048 diskretnih točk, in sicer tako, da smo za 512. diskretno točko dodali ničle. S tem smo izboljšali frekvenčno ločljivost iz 1,953 Hz pri 512 diskretnih točkah na 0,488 Hz pri 2048 diskretnih točkah. Frekvenčna ločljivost se je izboljšala za štirikrat. Slika 6 prikazuje ustrezno izračunano magnitudo spektrograma. Zaznati je izboljšanje jasnosti frekvenčne slike. Na tridimenzionalni sliki spektrograma je predvsem opazno enakomernejše naraščanje strmine grebena spektrograma. Na tlorisni projekciji se je zmanjšalo število kvadratnih struktur, ki jih vidimo na sliki 5 (tlorisna projekcija). Širina grebena se ni bistveno spremenila, kar je verjetno posledica nezmožnosti Gaussove okenske funkcije, da bistveno zmanjša pretakanje moči med sosednjimi frekvenca. Dodatno na širino grebena vpliva neustaljenost signala. Tudi na tej sliki vidimo, da so po 30 s magnitude spektrograma enake nič, kar je posledica dejstva, da smo v tem območju signalu dodali ničle.

Slika 7 prikazuje magnitudo skalograma horizontalnih pospeškov pralne grupe pralnega stroja pri zagonu. Skalogram je izračunan s frekvenčno ločljivostjo 1,953 Hz. Levi del slike prikazuje skalogram v prostoru, desni del pa tlorisno projekcijo. Na sliki lahko vidimo greben, katerega magnituda in frekvenca s časom naraščata. Tlorisna projekcija je zelo nejasna, tako da lahko zaznamo le zelo grob vzorec naraščanja frekvenca. Slika 8 prikazuje magnitudo skalograma, izračunanega s štirikrat boljšo frekvenčno ločljivostjo (0,488 Hz). Tako izračunana frekvenčna slika je bistveno jasnejša. Magnituda in frekvenca zelo lepo vidnega grebena s časom naraščata. Greben predstavlja magnitudo valčnih funkcij določene skale (frekvenca) in časovne premaknitve (časovni indeks). Greben je ozek, kar pomeni, da je odtokanje moči na sosednje frekvenca majhno. Tudi na tlorisni projekciji skalograma je naraščanje frekvenca lepo razvidno.

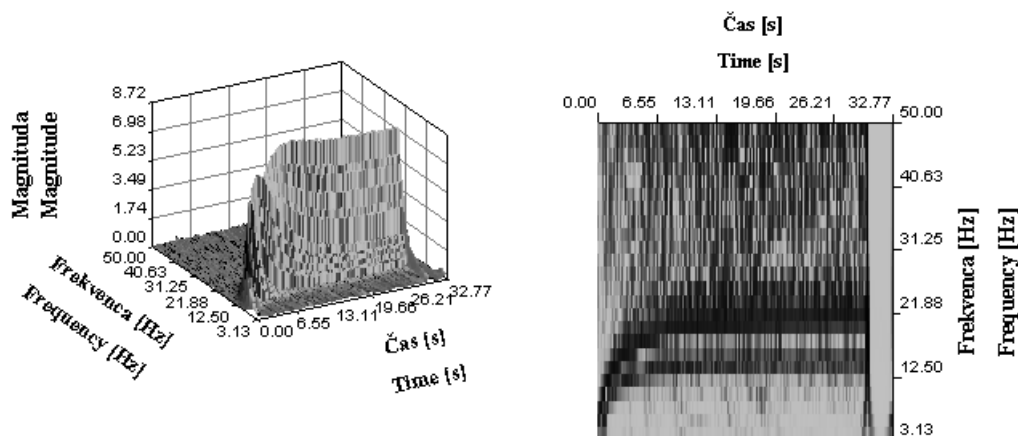
very unclear, this can be attributed to the low frequency resolution and the Fourier transform basic functions (sine and cosine). The power leakage could be reduced with the selection of a better window function but that would make it harder to compare spectrograms with scalograms. In this study a comparable Gaussian window function and Gabor wavelet were used which enabled us to compare the calculated spectrograms and scalograms.

Next, we tried to improve the readability of the 2D plots of the spectrogram. We increased the frequency resolution by appending zeros to the length of each window function. The window length was increased to 2048 discrete points. The frequency resolution increased by a factor of 4 (from 1.953 to 0.488 Hz). Figure 6 depicts the corresponding spectrogram. On the surface plot the slope of the ridge is more regular than before. The clarity of the 2D projection also improved, however, the width of the ridge was not changed significantly. The width of the ridge is proportional to the power leakage and the probable explanation could be that the Gaussian window function does not sufficiently reduce the power leakage. Since after 30 s only zeros can be found in the signal, the magnitudes of the spectrogram in this region are equal to zero.

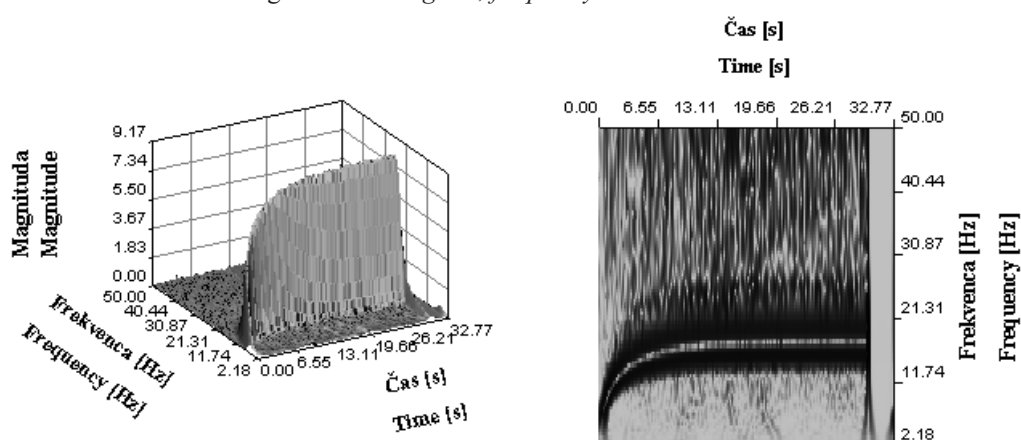
The scalogram magnitude of the washing-machine complex's horizontal accelerations during startup is shown in Figure 7. The left part of the picture shows a surface plot presentation while the right part shows a 2D plot of the scalogram. The scalogram is calculated with a frequency resolution of 1.953 Hz. Here again, the ridge with rising magnitude and frequency can be seen. The 2D projection is very unclear and only a coarse pattern of the frequency-time dependence can be observed. The scalogram magnitude with improved frequency resolution (0.488 Hz) is shown in Figure 8. The readability of the 2D projection has improved significantly. The magnitude and frequency of the ridge increase with time. The width of the ridge is small, suggesting small power



Sl. 6. Spektrogram, frekvenčna ločljivost 0,488 Hz
Fig. 6. The spectrogram, frequency resolution 0.488 Hz



Sl. 7. Skalogram, frekvenčna ločljivost 1,953 Hz
Fig. 7. The scalogram, frequency resolution 1.953 Hz



Sl. 8. Skalogram, frekvenčna ločljivost 0,488 Hz
Fig. 8. The scalogram, frequency resolution 0.488 Hz

Prikazano je frekvenčno območje od 2 Hz do 50 Hz. Po 30 s ni več nihanja, zato je magnituda skalograma v tem območju enaka nič.

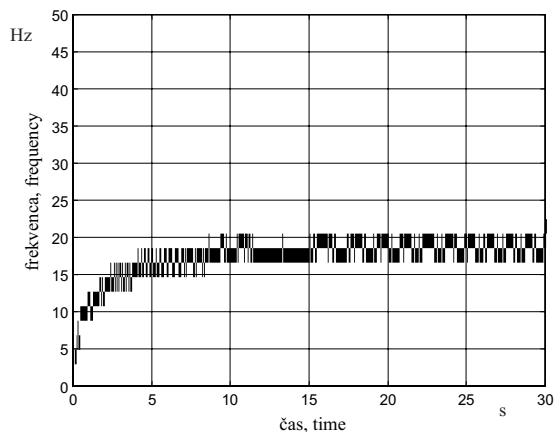
2.2 Primerjava grebenov spektrogramov in skalogramov

Na slikah 9 do 14 so prikazani grebeni spektrogramov in skalogramov horizontalnih pospeškov pralne grupe pralnega stroja. Na teh slikah so razlike med posameznimi načini izračuna frekvenčne vsebine še dodatno razvidne. Greben dobimo tako, da pri določenem časovnem indeksu prikažemo samo največje vrednosti magnitude spektrograma oziroma skalograma. Iz grebena spektrograma s frekvenčno ločljivostjo 1,953 Hz je skoraj nemogoče izluščiti vrednost frekvence pri posameznem časovnem indeksu. Greben spektrograma s frekvenčno ločljivostjo 0,488 Hz predstavlja izboljšanje, vendar je še vedno neberljiv. Navkljub izboljšanju frekvenčne ločljivosti se širina grebena ni bistveno zmanjšala. V nasprotju s prvima dvema greben skalogramov natančneje prikaže spreminjanje frekvence pri zagonu pralnega stroja.

leakage. The frequency range of the scalogram is 2 to 50 Hz. After 30 s there are no vibrations present, therefore the scalogram vanishes.

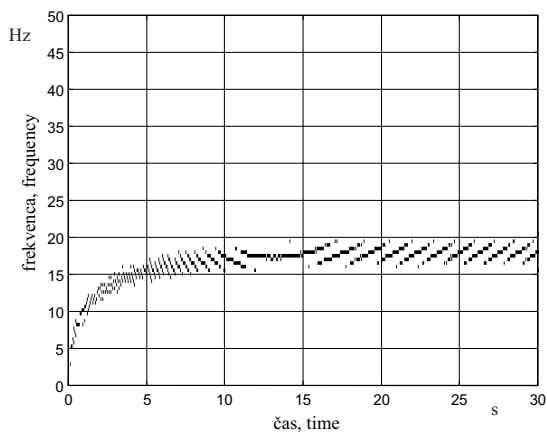
2.2 Comparison of the ridges of the spectrogram and scalogram

Figures 9 through 14 show spectrogram and scalogram ridges of the washing-machine complex's horizontal accelerations during startup. The differences between windowed Fourier and continuous wavelet analyses are here emphasized. The ridges are obtained when the maximum magnitude values of the spectrogram (scalogram) at a given time index are displayed. It is very difficult to determine the frequency-time dependence from the spectrogram ridge with a frequency resolution of 1.953 Hz. The spectrogram ridge with a frequency resolution of 0.488 Hz represents an improvement over the former ridge, but it is still difficult to read. In spite of the improved frequency resolution, the width of the ridge has not changed significantly. In contrast, the scalogram ridges are much more precise. The ridge scalogram, calculated with a frequency resolution of 0.488 Hz is



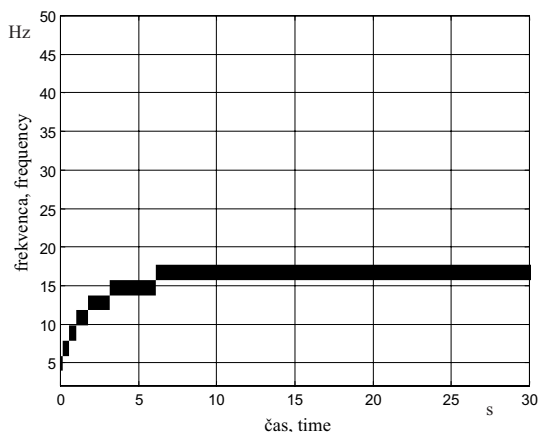
Sl. 9. Greben spektrograma, frekvenčna ločljivost 1,953 Hz

Fig. 9. The ridge of the spectrogram, frequency resolution 1.953 Hz



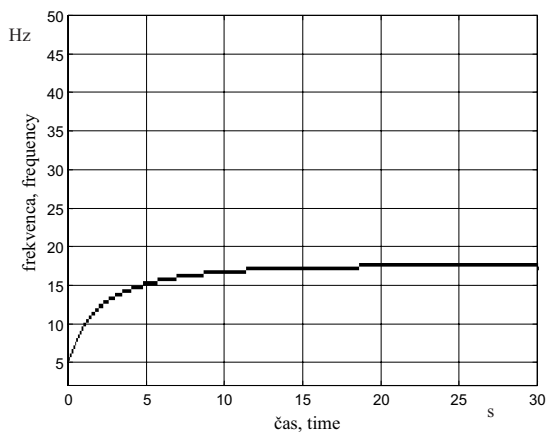
Sl. 10. Greben spektrograma, frekvenčna ločljivost 0,488 Hz

Fig. 10. The ridge of the spectrogram, frequency resolution 0.488 Hz



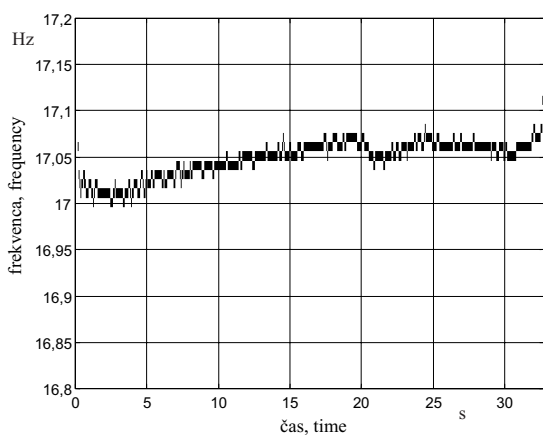
Sl. 11. Greben skalograma, frekvenčna ločljivost 1,953 Hz

Fig. 11. The ridge of the scalogram, frequency resolution 1.953 Hz



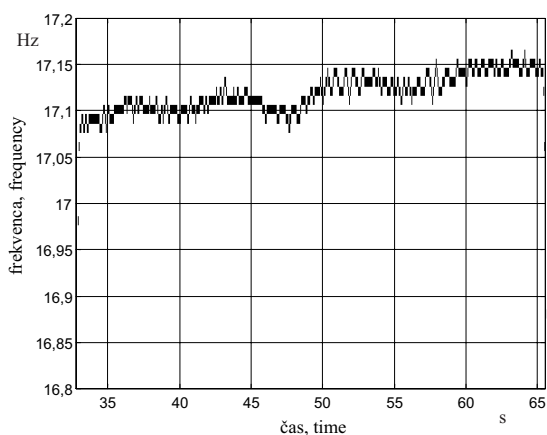
Sl. 12. Greben skalograma, frekvenčna ločljivost 0,488 Hz

Fig. 12. The ridge of the scalogram, frequency resolution 0.488 Hz



Sl. 13. Greben skalograma, ustaljeno stanje. Frekvenčna ločljivost 0,01 Hz

Fig. 13. The ridge of the scalogram, the stationary state. Frequency resolution 0.01 Hz



Sl. 14. Greben skalograma, ustaljeno stanje. Frekvenčna ločljivost 0,01 Hz

Fig. 14. The ridge of the scalogram, the stationary state. Frequency resolution 0.01 Hz

Natančnejši je skalogram, ki je izračunan pri frekvenčni ločljivosti 0,488 Hz. Frekvence na začetku ni mogoče zaznati iz dveh razlogov:

- Pri izračunu skalogramov smo se omejili na frekvenčno območje 2 do 50 Hz. Spremljanje frekvenčnega območja pod 2 Hz bi zahtevalo časovno bistveno daljše izračune.
- Pri izračunu grebena smo zanemarili vse vrednosti manjše od 1/20 največje vrednosti magnitude skalograma. Amplitude nihanja na začetku zagona so bile tako majhne, da so ustrezne vrednosti magnitude spektrograma padle pod postavljeni kriterij.

Frekvence vrtenja bobna, dobljene iz skalograma z boljšo frekvenčno ločljivostjo, so prikazane v preglednici 3. Frekvenčna ločljivost je 0,488 Hz. Po 12 s zagona se vrtilna frekvenca spreminja manj kot 3%. Pri 30 s je vrtilna hitrost 17,304 Hz, kar se zelo dobro ujema z že znanimi rezultati ([18] do [21]), pri katerih je bila izračunana vrtilna frekvenca ožemanja pri ustaljenem stanju 17,58 Hz.

2.3 Spreminjanje frekvence vrtenja bobna v ustaljenem stanju

Želeli smo tudi preveriti ustaljenost frekvence vrtenja bobna v ustaljenem stanju. Izračunali smo grebene skalogramov horizontalnih pospeškov pralne skupine v ustaljenem stanju. Pri merjenju pospeškov smo frekvenco vzorčenja povišali na 2000 Hz. Grebene smo izračunali s

the most precise of all the calculated ridges. At very small time indexes the ridges do not detect frequency for two reasons:

- Scalograms were calculated only in the frequency region of 2 to 50 Hz. Calculating scalograms at lower frequencies would be significantly more time consuming;
- When calculating ridges, all magnitudes lower than 1/20 of the maximum magnitude were ignored. The amplitude of the vibrations at the beginning of the startup fall below this criterion.

Drum-spin frequencies, extracted from the scalogram with a frequency resolution of 0.488 Hz, are presented in Table 3. After 12 s the frequency changes less than 3%. At 30 s the frequency is 17.304 Hz, which matches with previous studies ([18] to [21]). In these studies the dry spin frequency in the steady state was determined to be 17.58 Hz.

2.3 Spin frequency variation in the stationary state

The steadiness of the spin frequency in the steady state was checked. Scalogram ridges of the washing-machine complex's horizontal accelerations in the steady state were calculated. The signal of the horizontal accelerations was sampled with a higher sampling frequency, $f_s=2000$ [Hz]. Ridges were calculated with a

Preglednica 3. Spreminjanje trenutne frekvence pri zagonu pralnega stroja. Vrednosti grebena skalograma horizontalnih pospeškov. Frekvenčna ločljivost 0,488 Hz

Tabel 3. The instantaneous frequency during a washing-machine startup. Values of the scalogram ridges of the horizontal accelerations. Frequency resolution 0.488 Hz

čas v s time in s	1	2	4	6	8	10	12	14
frekvenca v Hz frequency in Hz	9,496	12,424	14,376	15,840	16,328	16,816	17,304	17,304
čas v s time in s	16	18	20	22	24	26	28	30
frekvenca v Hz frequency in Hz	17,304	17,304	17,304	17,304	17,304	17,304	17,792	17,304

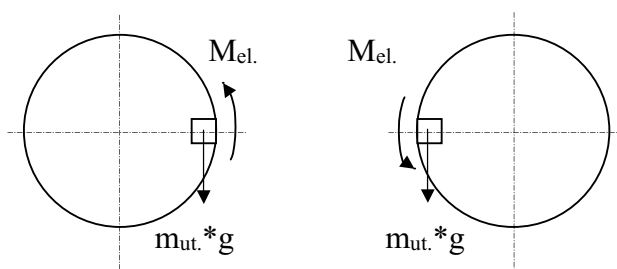
Preglednica 4. Podatki o parametrih izračuna grebenov skalogramov

Tabel 4. Ridge scalogram calculation data

valček wavelet	gabor
S_{\min}	2
σ	1,5
spodnja meja računanega frekvenčnega območja lower frequency bound	16 Hz
zgornja meja računanega frekvenčnega območja higher frequency bound	18,18 Hz
frekvenčna ločljivost frequency resolution	0,01 Hz

frekvenčno ločljivostjo 0,01 Hz. Podatki o izračunu grebenov skalogramov so podani v preglednici 4. Slika 13 prikazuje greben v časovnem območju 0 do 32,7675 s, slika 14 pa greben v časovnem območju 32,760 do 65,5355 s. Opazimo lahko, da frekvenca vrtenja bobna ni konstantna, temveč s časom počasni narašča. Pogonski elektromotor še naprej pospešuje vrtenje bobna. Z večanjem vrtilne frekvence se moment elektromotorja manjša. Posledično se zvečuje vrtilna frekvenca bobna vedno počasneje. Spreminjanja vrtilne frekvence bobna znotraj enega vrtljaja ni mogoče zaznati. To je v nasprotju s pričakovanji, saj se moment pospeševanja bobna znotraj enega vrtljaja spreminja (sl. 15).

frequency resolution of 0.01 Hz. Details of the calculations are given in Table 4. The scalogram ridge for the time period 0 to 32.7675 s is presented in Figure 13, while the scalogram ridge for the time period 32.760 to 65.5355 s is presented in Figure 14. It is evident that the spin frequency is not constant. The driving electromotor slightly accelerates the spinning of the drum and with increasing spin frequency the driving moment of the electromotor decreases. As a consequence, the spin frequency of the drum increases ever more slowly. Within one revolution the change in drum spin frequency cannot be detected. Because the driving moment, acting on the drum, depends on the instantaneous angle of the drum, we expected that the spin frequency within one revolution would not be constant.



Sl. 15. Vpliv lege uteži na moment pospeševanja bobna pralnega stroja

Fig. 15. The influence of the weight position on the washing-machine drum acceleration moment

3 SKLEP

V strojništvu pogosto želimo spremljati frekvenčno vsebino določenega procesa. Največkrat uporabljena metoda je izračun magnitude Fourierjeve transformacije. Zaradi svojih lastnosti je Fourierjeva transformacija primerna predvsem za spremljanje ustaljenih procesov. Pogosto pa se srečujemo tudi s neustaljenimi procesi. V teh primerih lahko spremljamo frekvenčno vsebino z uporabo integralnih transformacij, primernih za neustaljene procese. Med te transformacije štejemo okensko Fourierjevo transformacijo, Wigner-Villejevo porazdelitev, modificirane Wigner-Villejeve porazdelitve, valčno transformacijo. V tem prispevku sta prikazani okenska Fourierjeva in zvezna valčna transformacija. Njune zmožnosti spremljanja frekvenčnega vsebine neustaljenega procesa smo ugotavljali pri primeru zagona pralnega stroja.

Okenska Fourierjeva transformacija je omogočila grobo spremljanje frekvenčne vsebine. Odtokanje moči na sosednje frekvence je tako veliko, da so izračunani spektrogrami zelo nejasni. Izboljšanje frekvenčne ločljivosti z dodajanjem ničel v signal sicer izboljša jasnost, vendar je kakovost izračunane frekvenčne vsebine slabša kakor pri zvezni valčni transformaciji, izračunani z isto frekvenčno ločljivostjo. To je še posebej razvidno iz izračunanih grebenov, pri katerih spremljamo časovno spreminjanje vrtilne frekvence bobna pralnega stroja. Grebeni magnitude spektrogramov so zelo široki, posledično pa lahko

3 CONCLUSION

In mechanical engineering we often want to monitor the frequency content of a certain process. The most widely used method for monitoring frequency content is calculating magnitudes of the Fourier transform. However, due to the type of basic functions, the Fourier transform is only appropriate for stationary processes. Monitoring the frequency content of non-stationary processes requires the use of different methods. The windowed Fourier transform, the Wigner-Ville distribution, modified Wigner-Ville distributions and the wavelet transform are among methods that are appropriate for analyzing non-stationary processes. This paper deals with the windowed Fourier transform and the continuous wavelet transform. Their abilities for monitoring the frequency content of non-stationary process were studied for the case of a washing-machine startup.

Using the windowed Fourier transform we were only able to roughly determine the frequency content. The amount of power leakage resulted in very unclear spectrograms. Increasing the frequency resolution with zero padding did not significantly improve the readability of the spectrograms. On the other hand, scalograms calculated at the same frequency resolution as spectrograms offer better readability of the frequency content. This can also be seen in the figures of the ridges, which are used for determination of frequency-time dependence. The width of the spectrogram ridges is wide and the drum-spin frequency in the steady state

ugotovimo samo, da je vrtilna frekvenca bobna v ustaljenem stanju med 20,5 in 17 Hz. Z uporabo grebenov magnitude skalogramov lahko to napoved bistveno izboljšamo. Ugotovili smo, da je vrtilna frekvenca bobna v ustaljenem stanju 17,304 Hz. Preverili smo tudi samo ustaljeno stanje. Horizontalne pospeške pralne grupe v ustaljenem stanju smo ponovno pomerili, pri čemer smo uporabili višjo frekvenco vzorčenja. Grebene magnitud skalogramov ustaljenega stanja smo izračunali z bistveno boljšo frekvenčno ločljivostjo $-0,01$ Hz. Ugotovili smo, da se vrtilna frekvenca bobna ne ustali, temveč se s časom počasi zvečuje. Znotraj enega vrtljaja nismo zaznali spreminjanja vrtilne frekvence bobna.

Zahvala

Avtorji se zahvaljujemo Ministrstvu za šolstvo, znanost in šport za finančno podporo, ki jo dobivamo po pogodbi št. S24-782-007/19910/99.

can only be placed in the interval 17 to 20.5 Hz. This estimation of the drum spin frequency in the steady state can be improved on by using scalogram ridges, these ridges reveal that the drum spin frequency in the steady state is 17.304 Hz. In the next step the steady state itself was scrutinized. The washing-machine complex's horizontal accelerations in the steady state were measured using a higher sampling rate. The scalogram ridges were then calculated with a frequency resolution of 0.01 Hz. We determined that the drum spin frequency is not constant, but slowly increases with time. Within one revolution no variations in drum spin frequency could be observed.

Acknowledgement

The authors acknowledge the financial support of the Slovenian Ministry of Education, Science and Sport, contract No. S24-782-007/19910/99.

4 UPORABLJENE OZNAKE 4 USED SYMBOLS

koeficient	a_k	coefficient
koeficient	b_k	coefficient
koeficient	C_ψ	coefficient
frekvenca v Hz	f	frequency in Hz
funkcija v časovnem območju	$f(t)$	function in time domain
Fourierjeva integralska transformacija funkcije f	$\hat{f}(\omega)$	Fourier integral transform of $f(t)$ function
$f(k \cdot \Delta t)$	f_k	$f(k \cdot \Delta t)$
največja frekvenca v Hz	f_{\max}	maximum frequency in Hz
frekvenca vzorčenja v Hz	f_s	sampling frequency in Hz
okenska funkcija	$g_u(t) = g(t - u)$	window function
$\sqrt{-1}$	i	$\sqrt{-1}$
koeficient	k	coefficient
število diskretnih točk v signalu	N	number of discrete points in the signal
skala	S	scale
okenska Fourierjeva transformacija	$Sf(u, \omega)$	windowed Fourier transform
čas v s	t	time in s
perioda v s	T	period in s
parameter premika v s	u	time delay in s
Gaussova okenska funkcija	w_{Gauss}	Gaussian window function
valčna transformacija	$Wf(u, s)$	wavelet transform
časovni inkrement v s	Δt	time increment in s
koeficient	η	coefficient
koeficient	σ	coefficient
valčna funkcija v časovnem območju	$\psi(t)$	wavelet function in time domain
skalirana in translirana valčna funkcija	$\psi_{u,s}(t)$	scaled and translated wavelet function
Gaborjev valček v časovni domeni	ψ_{Gabor}	Gabor wavelet in time domain
Fourierjeva integralska transformacija $\psi(t)$	$\hat{\psi}(\omega)$	Fourier integral transform of $\psi(t)$
Fourierjeva integralska transformacija $\psi_{u,s}(t)$	$\hat{\psi}_{u,s}(\omega)$	Fourier integral transform of $\psi_{u,s}(t)$
Fourierjeva integralska transformacija ψ_{Gabor}	$\hat{\psi}_{Gabor}$	Fourier integral transform of ψ_{Gabor}
vektor diskretiziranega valčka	$\bar{\psi}_{k,s}$	discretized wavelet vector
frekvenca v rad/s	ω	frequency in rad/s
kompleksna konjugacija	*	complex conjugation
konvolucija	\otimes	convolution

5 LITERATURA
5 REFERENCES

- [1] Gabor, D. (1964) Theory of communications. *JIEE*.
- [2] Grossman, A., J. Morlet (1984) Decomposition of Hardy function into square integrable wavelets of constant shape. *SIAM Journal of Mathematical Analysis and Applications*, Vol. 15, No. 4, 723-736.
- [3] Boulahbal, D., M. Farid, F. Ismail (1999) Amplitude and phase wavelet maps for detection of cracks in geared systems. *Mechanical Systems and Signal Processing*, Vol. 13, No. 3, 423-436.
- [4] Lin, S.T., P. D. McFadden (1997) Gear vibration analysis by b-spline wavelet-based linear wavelet transform. *Mechanical Systems and Signal Processing*, Vol. 11, No. 4, 603-609.
- [5] Liu, B., S.-F. Ling (1999) On the selection of informative wavelets for machinery diagnosis. *Mechanical Systems and Signal Processing*, Vol. 13, No. 1, 145-162.
- [6] Paya, B.A., I. I. Esat (1997) Artificial neural network based fault diagnostic of rotating machinery using wavelet transforms as a preprocessor. *Mechanical Systems and Signal Processing*, 1997, Vol. 11, No. 5, 751-765.
- [7] Staszewski, W.J., S. Gareth Pierce, K. Worden, Wayne R. Philip, Geoffrey R. Tomlinson, B. Culshaw (1997) Wavelet signal processing for enhanced Lamb-wave defect detection in composite plates using optical fiber detection. *Optical Engineering*, Vol. 36, No. 7, 1877-1888.
- [8] Staszewski, W.J. (1997) Identification of damping in mdof systems using time-scale decomposition. *Journal of Sound and Vibration*, Vol. 203, No. 2, 283-305.
- [9] Staszewski, W.J. (1998) Identification of non-linear systems using multi-scale ridges and skeletons of the wavelet transform. *Journal of Sound and Vibration*, Vol. 214, No. 4, 639-658.
- [10] Ghanem, R., Romeo, F. (2000) A wavelet-based approach for the identification of linear time-varying dynamical systems. *Journal of Sound and Vibration*, Vol. 234, No. 4, 555-576.
- [11] Lamarque, C.-H., S. Pernot, A. Cueur (2000) Damping identification in multi-degree-of-freedom systems via a wavelet-logarithmic decrement-part 1: theory. *Journal of Sound and Vibration*, Vol. 235, No. 3, 361-374.
- [12] Hans, S., E. Ibraim, S. Pernot, C. Boutin, C.-H. Lamarque (2000) Damping identification in multi-degree-of-freedom systems via a wavelet-logarithmic decrement-part 2: study of a civil engineering building. *Journal of Sound and Vibration*, Vol. 235, No. 3, 375-403.
- [13] Staszewski, W.J., J. Giacomini (1997) Application of the wavelet based frfs to the analysis of nonstationary vehicle data. *Proceedings of the 15th International Modal Analysis Conference-IMAC*, Vol. 1, No. 4, 425-431.
- [14] Basu, B., V. K. Gupta (1999) Wavelet-based analysis of the non-stationary response of a slipping foundation. *Journal of Sound and Vibration*, Vol. 222, No. 4, 547-563.
- [15] Basu, B., V. K. Gupta (1999) On equivalent linearization using wavelet transform. *Journal of Vibration and Acoustics*, Vol. 121, 429-432.
- [16] Berger, B.S., I. Minis, J. Harley, M. Rokni, M. Papadopoulos (1998) Wavelet based cutting state identification. *Journal of Sound and Vibration*, Vol. 213, No. 5, 813-827.
- [17] Mallat, S. (1999) A wavelet tour of signal processing. *Academic Press*, 2nd Edition.
- [18] Jakšič, N. (1997) Analiza nihanja nelinearnega centrifugalno vzbujanega ravninskega sistema, *Univerza v Ljubljani, Fakulteta za strojništvo*, magistrsko delo.
- [19] Simonovski, I. (1998) Uporaba spektrov tretjega reda pri analizi nelinearnih mehanskih nihanj. *Univerza v Ljubljani, Fakulteta za strojništvo*, magistrsko delo.
- [20] Jakšič, N., M. Boltežar, I. Simonovski, A. Kuhelj (1999) Dynamical behaviour of the planar non-linear mechanical system - Part I: Theoretical Modelling. *Journal of Sound and Vibration*, Vol. 226, No. 5, 923-940.
- [21] Boltežar, M., N. Jakšič, I. Simonovski, A. Kuhelj (1999) Dynamical behaviour of the planar non-linear mechanical system - Part II: Experiment. *Journal of Sound and Vibration*, Vol. 226, No. 5, 941-953.

Naslov avtorjev: mag. Igor Simonovski
doc.dr. Miha Boltežar
Fakulteta za strojništvo
Univerze v Ljubljani
Aškerčeva 6
1000 Ljubljana

Authors' Address: Mag. Igor Simonovski
Doc.Dr. Miha Boltežar
Faculty of Mechanical Eng.
University of Ljubljana
Aškerčeva 6
1000 Ljubljana, Slovenia

Prejeto: 18.12.2000
Received:

Sprejeto: 12.4.2001
Accepted: